

# Computer-Enhanced Frequency-Domain and 12-Lead Electrocardiography Accurately Detect Abnormalities Consistent With Obstructive and Nonobstructive Coronary Artery Disease

Melvin B. Weiss, MD,\* S. Murthy Narasimhaidevara, MD,\* Gen Quan Feng, PhD,† and Joseph T. Shen, MD†

Noninvasive methods of identifying coronary artery disease are not consistently accurate. To identify abnormalities associated with angiographically determined coronary artery disease, the authors sought to quantify the utility of a new device, a digital database-driven multiphase electrocardiograph system (3DMP), which produces a computer-enhanced frequency/time-domain resting electrocardiogram, in conjunction with a 12-lead electrocardiogram. The authors compared resting 3DMP results from those of coronary angiograms to identify abnormalities associated with coronary artery disease in a random sample of 136 patients. Using a discrete-Fourier transform signal-averaging variant and a series of mathematic transformations, the computer-expert system analyzed signals in the 0.1- to 50-Hz range. The system identified abnormalities by comparing results with a 21,000-patient database culled from predicate research. The system detected abnormalities in 96.0% of patients subsequently found to have 70% or greater stenosis by angiography. For patients with a 40% or less times a more than 50% occlusion, the system detected abnormalities in 75% of cases. For patients with a 50% or less times a 70% or less occlusion, it detected abnormalities in 90% of cases. Overall sensitivity for the study was 93.3% (positive predictive value, 91.2%; specificity, 83%; negative predictive value, 86.7%). No gender differences were detected. A 3DMP electrocardiograph system combined with 12-lead electrocardiography appears to have measurable, diagnostic utility in identifying 3DMP abnormalities associated with coronary artery disease, and warrants further study.

Coronary artery disease (CAD) and its associated pathologies continue to affect patients worldwide. Cardiac illnesses remain the leading cause of death among Americans, accounting for 476,124 or 20.54% of all deaths in 1996.<sup>1</sup> The accurate, noninvasive detection of anomalies due to CAD continues to pose challenges to physicians. For example, although clinicians routinely use the electrocardiogram as an initial means of screening for gross cardiac

anomalies, the low sensitivity of this method makes it a poor diagnostic indicator of existing CAD.<sup>2</sup>

The use of invasive procedures for asymptomatic patients based on results of noninvasive testing remains controversial. Although minimally invasive modalities (e.g., thallium-201 stress tests) or truly invasive measures (e.g., coronary angiograms) accurately identify some form of myocardial stress, they pose additional risks to the patient. For example, to achieve 90% or greater sensitivities for nuclear stress modalities (i.e., thallium 201 and sestamibi), 70% or greater stenosis is needed. Other researchers have historically reported a diagnostic deficit owing to interobserver inconsistencies and poorer specificities.<sup>3,4</sup> Given only an anatomical perspective, angiograms seem to have questionable prognostic capacity.<sup>5,6</sup> Angiography may better serve patients when complemented with other modalities

Heart Disease 2002;4:2-12

Copyright © 2002 Lippincott Williams & Wilkins, Inc.

From the \*Division Of Cardiology, New York Medical College, Valhalla, New York; and †Cardiotron, LLC, Port Washington, New York.

Address correspondence and reprint requests to Joseph T. Shen, MD, Premier Heart, LLC, 14 Vanderverter Avenue, Suite 138 Port Washington, NY 11050; E-mail: jtsbenmd@premierheart.com

**TABLE 1**

Extrinsic factors influencing myocardium function

K <sup>+</sup> Levels	Valvular changes
Ca <sup>++</sup> Levels	Physical activity
Vascular tone	Serum pH
Respiratory rate	Heart rate
O <sub>2</sub> Concentration	RBC volume
K <sup>+</sup> Channel configuration	Renal regulatory influences
Myocardial cell perfusion	Neuroendocrinologic influences
Thoracic electromyographic activity	Myocardial and septal influx, efflux tracts

that provide a more thorough clinical view of cardiac dysfunction. Although promising strides have recently been made to detect ischemia at rest, the invasive radiologic means used to achieve this result could prove intimidating to the average patient. Angiography has a low but nevertheless significant risk of mortality.<sup>7-10</sup>

Furthermore, a thallium-201 stress test or angiography is only clinically indicated if a less-sensitive modality (e.g., resting or stress electrocardiogram) reveals some remarkable trait, such as increased S-T segment elevation or depression, Q-wave abnormalities, or other subtleties. Expert consensus and evidence now support the once-controversial premise that whereas nonobstructive disease is found in only a small number of patients undergoing angiography, these mild or moderate narrowings are the most likely causes of future clinical events.<sup>11-13</sup> However, Smith et al<sup>14</sup> recently highlighted strategies to identify low-, intermediate-, and high-risk patients from the population at risk for CAD, and offered several means to achieve these goals. They advocated shifting from diagnosis to prognosis and the use of noninvasive modalities, such as the ankle-brachial pressure index or electron-beam computed topography.

Clearly, the ideal environment for both the treating physician and the patient is a noninvasive one that measures end-organ (myocardium) intrinsic electromechanical reactivity to extrinsic factors (Table 1) quantitatively and at rest. The less-sensitive nature of resting and stress electrocardiograms indicates that they may not be able to diagnose all cases of CAD. Other noninvasive methods, such as signal average/late potential electrocardiography or electron-beam computed topography, seem better suited for specific niches. Electron-beam computed topography may more aptly be used as a screening method rather than a true diagnostic tool, despite limited utility that may show its ability to stratify CAD severity, whereas signal average/late potential electrocardiography can effectively identify patients at risk for sustained ventricular tachycardia.<sup>15-19</sup>

Both conventional and signal-average electrocardiography rely on time-domain analysis, which has been of limited use in the correlation of low heart-rate variability and risk of ventricular tachycardia.<sup>20,21</sup> Additionally, some efforts have been made using frequency-domain electrocardiography to identify the foci of myocardial dysfunction.<sup>22,23</sup> However, no major coordinated effort has used frequency-domain and power-spectrum analyses to identify abnormalities due to CAD.

Prasad et al<sup>24,25</sup> investigated a phase-invariant signature algorithm converting time-domain electrocardiograph signals to a phase domain and determined the accuracy in detecting canine ischemic conditions. This technique is distantly related to the multiphase frequency-domain analysis used in the current study. Another distantly related technique is power bispectral analysis of electroencephalographic signals (developed by Aspect Medical Systems), which involves the simultaneous capture and spectral analysis of two channels.<sup>26</sup> Bonato et al<sup>27</sup> have commented on the capacity of frequency-domain analysis to identify late potentials. Although their aim focused on late potential, and the highlighted sampling techniques have subsequently proven limited, similar techniques to maximize the signal-to-noise ratio and to optimize the waveform resolution are explicated and, in part, reflect the ability of this device to do the same.

The device compared in this study uses a database collected during approximately 8 years (1978-1986) of trials conducted in the People's Republic of China.<sup>28</sup> After the initial database was constructed, broader clinical investigations were conducted throughout Europe and North America (from 1989 to the present) to optimize the data application, and at one point involved 30 hospitals; the bulk of the 21,000 patients were culled from these trials.

#### **THEORETICAL AND PHYSIOLOGIC BASIS: HISTORICAL PERSPECTIVE**

Research regarding the foundations of this device began in 1976 (Fig. 1). The testing hypothesis that initiated the investigation and subsequent research was that chronic exposure to excessive noise had adverse, systemic effects on human cardiac function. At that time, no sufficiently sensitive and objective means of cardiology assessment for such an investigation existed. Electrocardiographic analysis was found to be inadequate because although previous clinical observations were found to correlate with noise exposure, electrocardiogram waveforms were consistently unremarkable.

The workers began by constructing a mathematic model of the myocardium and blood. Approximately 4 years of theoretical research were dedicated to combining the mathematic formula and the theoretical foundation for the initial design and construction of the system. Although database-driven clinical application was a future goal, the immediate aim was accurate forward transformation from the electrocardiogram analogue. Workers succeeded in their initial efforts to detect differences in forward-transformed digitized electrocardiographic data between control and experimental groups. Test and control groups were investigated in double-blind trials, and results were published in peer-review journals (Fig. 1).

Subsequently, animal trials were conducted on both rodent and canine subjects. Although the only basic means of coronary ligation available were for canine subjects, experimentation yielded positive results and pointed to the need for further exploration. The same results were also reproduced in magnesium-sulfate infusion studies in rodents. Starting in 1980, the workers concurrently began a success-

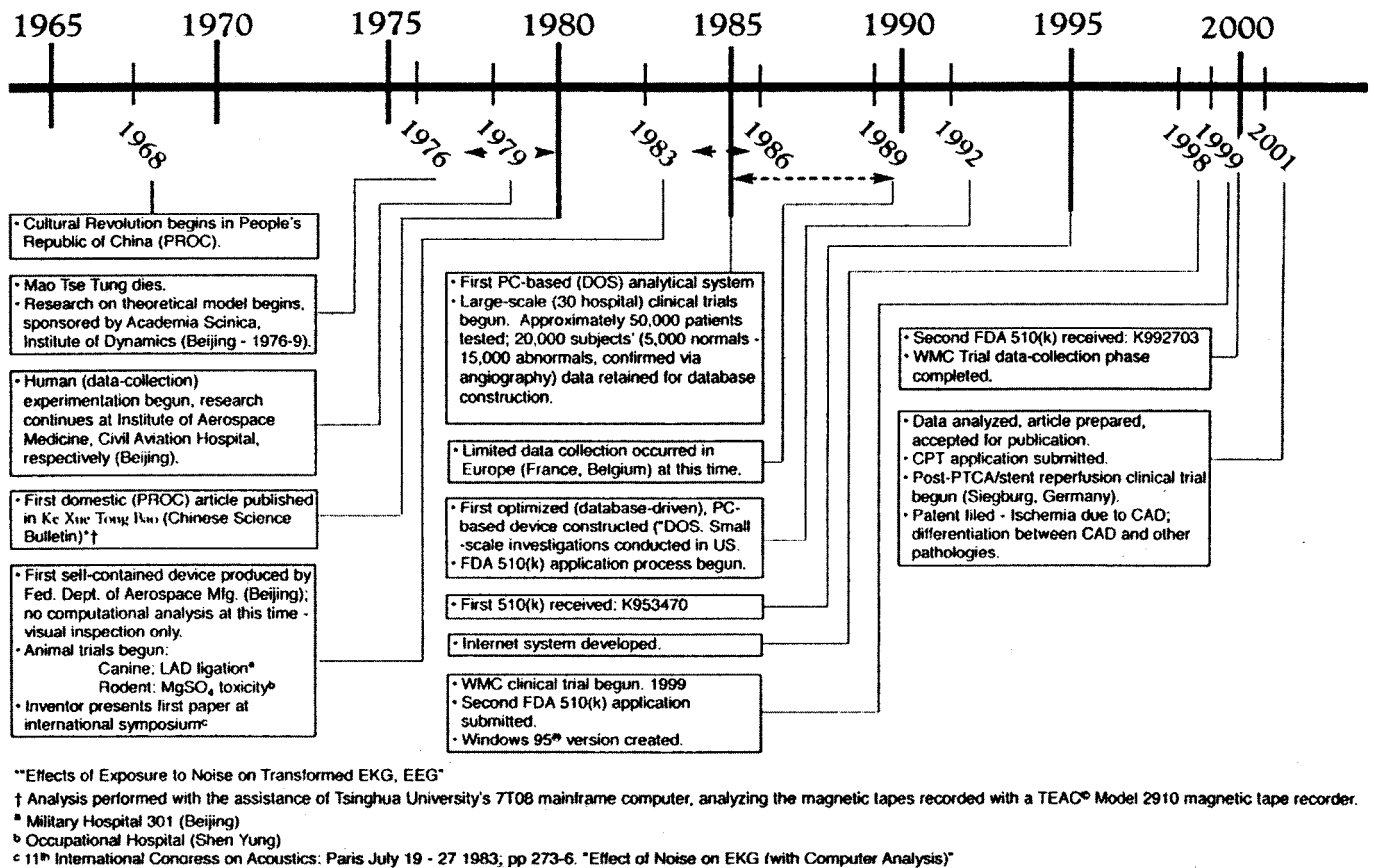


Figure 1. Timeline of pertinent historical events.

fully conducted pilot study investigating the capacity of the device to measure the changes from the forward-transformed, digitized electrocardiographic data from three distinct groups of patients with distinct clinical outcomes.

Historically, Einthoven presumed the myocardium to be a single-point electrical generator, without empirical or experimental evidence to make this conclusion. The creators of the 3DMP electrocardiograph thought otherwise, and began by using two mathematic descriptions of two intrinsic physiologic properties of the heart. First, the myocardium is a viscoelastic solid. Second, blood is non-Newtonian fluid at low and intermediate shearing states. These two relations have been generally accepted by physiologists worldwide. The Frank-Starling rule, bridging the relation between venous return and myofibril length with adenosine triphosphate- and ion-driven actin-myosin interactions at its root, provided a physiologic basis for the electromechanical relations behind the adoption of biocybernetic concepts that lie in this device's theoretical approach to mathematic modeling of the myocardium.<sup>29-31</sup> Third, to unify these two intrinsically physiologic properties, the investigators proceeded to fuse these two mathematic relations into one by using Laplace transform. This approach may be the most important contribution to the field of biomimetics, and lays a foundation for other applications and advancement in similar fields (e.g., electroencephalography, electromyography, nanotechnology).

The formulas used to describe a functioning myocardium are complex and beyond the scope of this article.

Briefly, three major formulae are used to describe 1) the myocardium and its interactions with the blood, a viscoelastic solid subject to dynamic stress-strain module and nonlinear elasticity variables; 2) blood as a non-Newtonian or usually compressible fluid that acts as a Newtonian fluid only at high shear; and 3) the fusion of these two concepts into a third function that also depicts the myocardium as a series of concentric energy shells interacting with the venous return from cycle to cycle, and provides boundaries for these shells during systole and diastole. This fundamental interaction provides the basis for measuring the complex interactions of the heart with other extrinsic factors (Table 1).

The following theoretical postulates were conceived when combined with experimentation for these formulae: 1) the heart is a nonlinear system; 2) simultaneous sampling and computing of at least one pair of leads, representing the input and output of a system, is necessary<sup>31</sup>; 3) selection of these particular six mathematic transformations (from an array of > 100 fast-Fourier transforms) may be useful in electrocardiographic signal analysis; 4) any complex system may have information that cannot be completely expressed by any single set of coordinates; 5) different coordinate planes may express information that other coordinate systems cannot; 6) integrated results of clinically tested and relevant indices are greater than the sum of a portion or all of the indices extracted from the system; and 7) indices discovered during research (i.e., heart disease) need to be

$$\begin{array}{ll}
 \text{A]} & G_{xx} = S_x(f) \cdot S_x(f)^i \\
 & G_{yy} = S_y(f) \cdot S_y(f)^i \\
 \text{B]} & T_{xy} = G_{xx}/G_{yy} \\
 \text{C]} & P_{ih} = F^{-1}T_{xy} \\
 \text{D]} & \gamma^2 = \frac{G_{xy}^2}{(G_{xx})(G_{yy})} \\
 \text{E]} & V_{xy} = F^{-1}G_{xy} \\
 \text{F]} & \theta_{xy} = \tan^{-1} T_{xy(I)}/T_{xy(R)}
 \end{array}$$

**Figure 2.** Six mathematical (power spectrum) transformations.

repeatedly tested to establish their clinical importance and relevance.

The approach researchers chose stems from approximately 5 years of refinement of the set of mathematic principles, and the reproducible patterns extracted from the repeated observations stemming from the large-scale, double-blind trials, into the database on which the software was built. A technical article that explores these concepts in more detail is forthcoming. Again, the computer is used to categorize cardiac dysfunction. The following explanations provide for general phenomena that may be evident on visual inspection, yet the more than 132 indices have been identified from the transformations and used in the software for differentiation. Since the 1990s, new indices and thresholds have been discovered and integrated into the software for further optimization.

## THE SIX MATHEMATIC TRANSFORMATIONS

All of the mathematic transformations are based on the power spectrum ( $G_{xx}$ ,  $G_{yy}$  for leads  $V_5$  and II, respectively). The power spectrum uses both real and imaginary number sets, where the domain of the coordinate plane is the set of real numbers [R] and the range encompasses the imaginary number set [I]. The autopower spectrum remains within the respective lead ( $V_5$  or II), and the cross-power spectrum ( $G_{xy}$ ) is used when attributes of each lead are to be compared. Note the subscript changes.

The autopower spectrum, (Fig. 2, formulae A) depicts the power distribution along a frequency range of 0.1 to 50 Hz.  $G_{xx}$  is obtained from  $V_5$ , whereas  $G_{yy}$  is obtained from lead II. Empirical observation has elicited patterns among the six transformations that have consistently appeared with specific patient conditions. Although the power spectrum and its derivatives used by the 3DMP electrocardiograph are usually reserved for physics applications (coherence, impulse response, transfer function phase angle shift, cross-correlation, and amplitude histogram), these otherwise electromechanical terms were adopted, refined, and applied to biologic systems.

The analysis of the data from over 21,000 patients lead researchers to conclude that the first peak represents the fundamental frequency of the heart, which is 1 Hz. Subsequent harmonics may represent the intrinsic frequencies of different myocardial structures of differing sizes and architecture from different layers of myocardium.

Our efforts established that approximately 80% of the power exerted by the myocardium is represented in the first 10 peaks of the power spectrum graphs. For example, al-

**TABLE 2**  
Diagnostic codes

### Diagnostic codes

A:	ventricular hypertrophy or hypertensive heart disease
C:	ischemic heart disease due to CAD, anemia, etc.
C(I):	ischemic heart disease and potential MI
M:	ischemic heart disease, cardiomyopathy
DKIC:	differentiation between K and C
DVBT:	differentiation between V and T
F:	rheumatic heart disease, including valvular involvement
G:	congenital heart disease
K:	myocarditis
N:	atrial fibrillation
T:	premature atrial contraction
T1, T2, T3, T4:	Four sequential symbols with no clinical meaning
U:	cor pulmonale
V:	ventricular fibrillation

CAD = coronary artery disease; MI = myocardial infarction.

terations in peak amplitude ratios are thought to represent the redistribution of power among the peaks (or harmonics) owing to alterations in myocardial power output from its various components caused by one or more known pathologic entities (Table 2), though the focus for this peer review is limited to CAD.

Transfer function, represented by  $T_{xy}$  (Fig. 2, formula B), has two components or phases. As noted in the table, dividing cross-power spectrum ( $G_{xy}$ ) by autopower spectrum ( $G_{xx}$ ,  $G_{yy}$ ) yields two complementary components or phases of the frequency and power axes, namely amplitude and phase angle. The amplitude of this result is referred to as the transfer function. Transfer function is a measure of deviations away from 1, where 1 is the ideal ratio between  $G_{xy}$  and  $G_{xx}$ . Deviations below or above 1 may reflect myocardial abnormalities related to hypertrophied myocardial disease of various causes. This function has just recently come into focus for practical applications, and was not used in the older versions of the software (i.e., before 1990).

Phase angle shift (Fig. 2, formula F) is the arctangent of the dividend between the imaginary and real number sets and indicates both global and localized synchronization between the fields captured by the two leads. Degrees are used to denote out-of-phase leads (maximum,  $\pm 180^\circ$ ).

Myocardial compliance is illustrated in the impulse-response graph, the inverse ( $F^{-1}$ ) of the transfer function (Fig. 2, formula C). Taking the inverse reverts the coordinate plane back to the time domain. Contrary to conventional views of modern physiology, the effect of increased compliance (conveyed through indices such as those shown in Figure 3) on impulse response has been observed to reflect ventricular tachycardia/fibrillation, ventricular dilatation, ischemia, and overall system quality. Decreased compliance may indicate left-ventricular hypertrophy and global or local myocardial hibernation, or damage due to ischemia or infarct.

The results from coherence produce a unit value,  $\gamma^2$  (Fig. 2, formula D). This unitless number reflects the net disparity between the cross-power spectrum and the product of the two power spectra of leads II and  $V_5$ . The distortion of the myocardium away from a threshold value ( $\approx 0.68-0.71$ ) is reflected here. This is a universal threshold of degree of coherence for the myocardium at the system's fun-

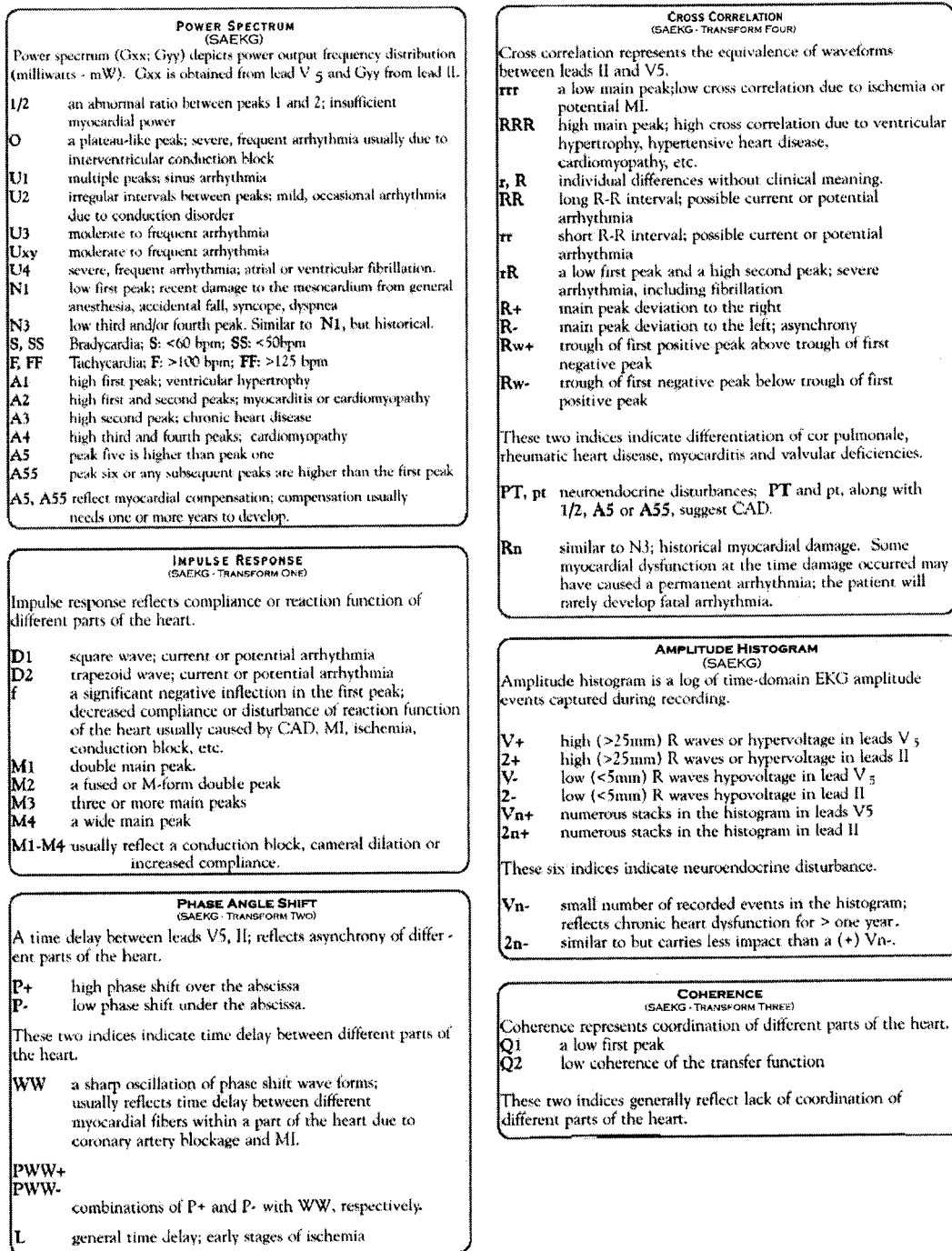


Figure 3. 3DMP index listing.

damental frequency of any physical, chemical, or biologic system. A value of 1 would indicate a theoretically perfect spherical order (where phase, amplitude, and frequency are coherent), whereas a value of 0 is undefined and clinically represents ventricular fibrillation.

The sixth transformation, cross-correlation, is the reciprocal of cross-power spectrum (Fig. 2, formula E). Only the shared qualities of both leads are studied here. The commonalties of both leads are compared during one 5.12-second cycle and this inversion is reflected in the cross-correlation graph, with 2.56-seconds representing the extent of the abscissa on either side of the y-axis.

The 3DMP electrocardiogram has achieved a new milestone in the differential diagnosis of CAD. These current clinical efforts focus on CAD and its sequelae, though patterns consistent with ischemia due to other causes or other nonischemic heart diseases (OHD) are noted. Furthermore, OHD investigations are part of a continuing effort to discern their patterns using the 3DMP electrocardiograph.

The present study is the first in North America to verify the accuracy of the 3DMP electrocardiography computer-expert system. The system adopts the following three principal means: 1) it uses a rational means of processing electrocardiograph signals to optimize signal-to-noise ratio

and waveform resolution, based on cybernetic and Nyquist principles at a lower sampling rate than conventional methods (at 100 points/s); 2) it also applies a mathematically derived physiologic model with six mathematical transformations following discrete-Fourier transform after signal digitization; and 3) it extracts information from a database of indices collected from previous investigations to determine if it can identify altered 3DMP expressions registered on some or all of the six mathematics functions for the myocardium. Detectable at resting conditions, the abnormal expressions were found to be consistent with patients experiencing chronic imbalance between myocardial demand and coronary artery supply due to the onset of CAD, beginning with 40% narrowing. It also identifies the abnormal expressions consistent with more acute conditions with greater percent-grade narrowing and subsequently higher stress placed on this supply-demand imbalance.

## METHODS

Subjects were ambulatory patients who presented at Westchester Medical Center in Valhalla, NY. Based on varied modalities including current symptoms, history, and physical examination findings, patients were considered for diagnostic coronary angiography. The selection process relied entirely on clinical judgment; physicians used tools commonly at their disposal (e.g., hematologic assays, chief complaint, 12-lead electrocardiogram findings) and had no knowledge of whether the patient was a candidate for study. The specific intent was not to assess the capacity of the 3DMP electrocardiogram as a screening device at this time, but instead to focus primarily on its potential as a diagnostic assay.

Patients were excluded if they had contraindications to angiography (e.g., reactivity to intravenous contrast), a history of cardiac surgery (e.g., coronary artery bypass graft, percutaneous transluminal coronary angiography), long-term drug abuse, or if they were pregnant.

Interventional cardiologists, blinded to 3DMP electrocardiogram results and clinical information, performed coronary angiography according to Westchester Medical Center angiography procedure and trial protocols. Demographic information; vital signs; and surgical, medical, family, and social histories were recorded. Current medication, laboratory values, and follow-up information were obtained before coronary angiography was performed. The 3DMP device was blinded to all of these data.

Patients were instructed to lie in the supine position and rest for 20 minutes to minimize the musculoskeletal motion noise and hemodynamic or neurohormonal influences to the heart. Five electrodes occupied typical positions on the patient ( $\approx 2$  in above the medial malleolus and  $\approx 1.5$  in above the radial crease on both arms). The precordial lead,  $V_5$ , was placed in the conventional position at the fifth intercostal space at the intersection of the anterior axillary line. This process uses a discrete-Fourier transform signal-processing variant and a series of six mathematic transformations, such as power spectrum, phase-angle shift, impulse response, transfer functions, amplitude histogram,

**TABLE 3**  
Calculated overall sensitivity and specificity

Legend	Sn	93.26%
$n = 136(n_m = 79, n_f = 56)$		
age $\bar{x}_m = 60.2, \sigma = 12.3$ years	Sp	82.98%
$\bar{x}_f = 63.0, \sigma = 12.4$ years	PPV	91.21%
	NPV	86.67%
Sensitivity = (Sn)		
Specificity = (Sp)		
Pos. Predictive Value = (PPV)		
Neg. Predictive Value = (NPV)		

and cross-correlation (Fig. 2). The results of all the positive indices of the six transformations were identified and integrated into a single pattern. Abnormalities were identified by comparing the results to a 21,000-patient database culled from predicate research.

Angiographic data were visually analyzed according to the BARI (bypass angioplasty revascularization investigation) coronary angiographic scoring system.<sup>32</sup> The abnormalities stemmed from angiographically determined non-obstructive CAD (single-vessel arterial narrowing of  $\approx 40\% \leq x < 70\%$ ) to obstructive CAD (single-vessel or multivessel arterial narrowing of  $\approx 71\text{--}100\%$ ), with the exception of the left main, where 50% or greater narrowing is considered obstructive. Normal is defined clinically as patients who have less than 40% narrowing or no angiographic narrowing.

An approximately 95% musculoskeletal artifact-free dataset is required for analysis. Ambient artifact or noise may stem from an inadequately prepared skin surface, loose or unsecured electrodes or alligator clips, contiguous electrocardiogram leads or those contiguous with a metal surface other than the device (e.g., examination table, patient bed or gurney), or poor ground.

As required by discrete-Fourier transformation, we broke the 82-second span into 16 segments of 5.12 seconds each. The device is only minimally tolerant of incidental patient movement and must be readministered if the waveform exceeds the following limits (waveforms outside of the following were readministered):

1. If the waveforms represented in five or more segments contain idiopathic extrema, which deviate  $\geq 2$  mm from the baseline and appear more than 10 times;
- 2a. If two or more segments show idiopathic extrema that deviate from the 5-mm baseline;
- 2b. If the waveform strays from the baseline by  $\geq 3$  mm within a 25-mm section of waveform represented in any one of the 16 segments;
3. If the waveform shows a radical deviation of  $\geq 2$  mm from the baseline  $80 \pm 10^\circ$  two or more times, or a single episode of  $\geq 5$  mm.

Results were interpreted manually from combined clinician interpretation of specific 12-lead electrocardiogram elements and the automatic computer analysis. Any of the criteria normally observed when interpreting a 12-lead electrocardiogram were also noted here. Phenomena such as T-wave inversion, S-T segment changes, Q-wave abnor-

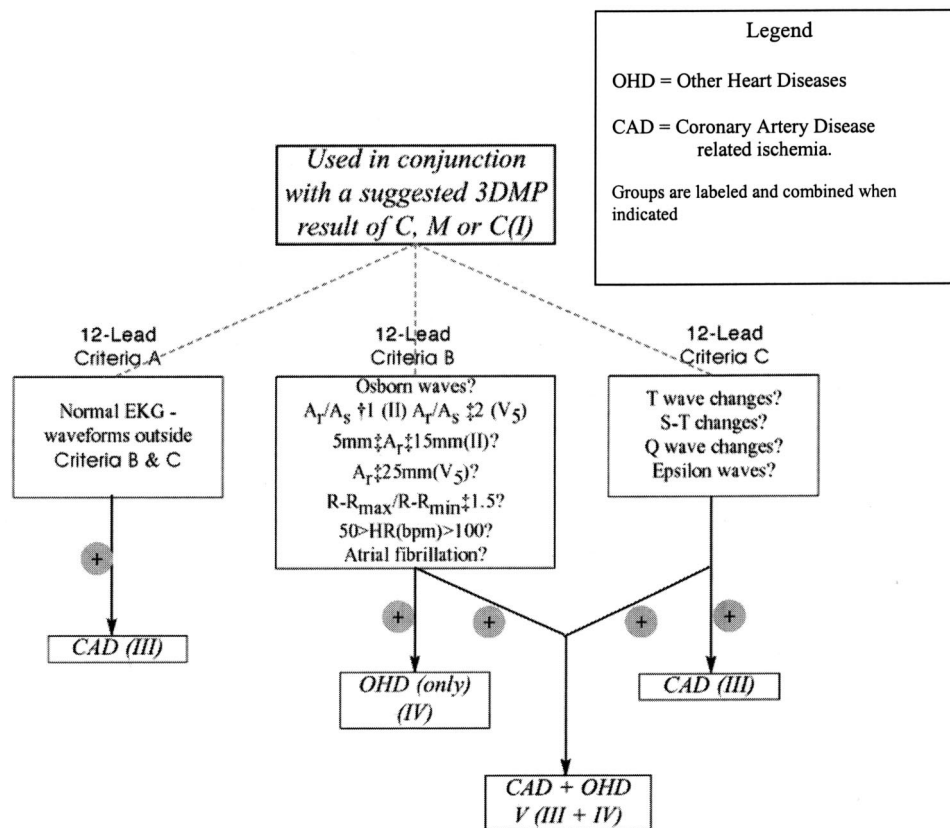


**Figure 4.** Flowchart to aid differential diagnosis.

malities, long Q-T interval, and short PR segment attributed to Wolff Parkinson White syndrome all remain valid. Figure 4 displays a flowchart or decision tree to determine patient results. Patients meeting corresponding criteria for pathway A, B, or C would then be classified in the subsequent diagnoses. The differentiation between CAD and other diseases is done automatically, and disease severity can also be analyzed automatically. Figure 5 shows tracings from patients (not enrolled in this study) that reveal distinct patterns that 3DMP electrocardiogram researchers have used to classify normal, moderate, and severe categories. Set A is from a 73-year-old man determined to have severe yet asymptomatic triple-vessel disease (left main, 50%; left-anterior descending, 99%; left circumflex, 80%). Set B shows moderate disease in an asymptomatic 66-year-old man (left-anterior descending, 40–50%; left circumflex, 50%). Graph set C shows a normal, 18-year-old man. All had normal resting/stress electrocardiogram findings. Although graphic differences are apparent, more objective digital indices are used to classify patients.

Actual sample time lasted approximately 82 seconds. Two tests were performed whereby two leads, II and V<sub>5</sub>, were simultaneously captured. Before, during, and after the first 82-second test, no clinical or historical patient information was recorded, which established an objective position by which the machine generated a suggested diagnoses based on the myocardial signal received.

An isolation transformer was used to prohibit a 60-cycle hum from interfering with tracings, and a 20-minute rest and a placid environment were strictly adhered to. Exami-

nation rooms were used whenever necessary to keep the number of personnel in the area to a minimum.

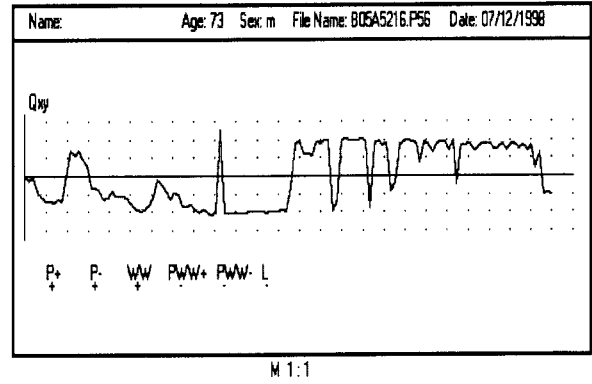
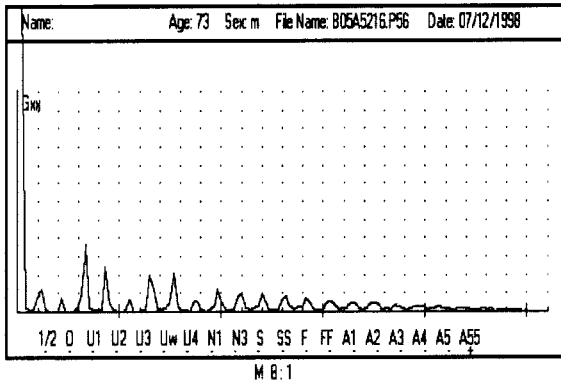
## RESULTS

A total of 200 patients were selected for study, though readings were only obtained from 136 patients (68%). This rate was attributed to several factors: 1) tracings that were free of kinetic and electromagnetic field artifact were difficult to obtain in high-volume ambulatory-care settings; 2) patient anxiety levels produced by the locale; 3) musculo-skeletal artifact or rapid breathing, again attributable to anxious patients or Parkinsonian/dystonic tremor; and 4) isolation transformers minimized but occasionally did not eliminate 60-cycle hum from the occasional unshielded electrical outlet located in older areas of the facility.

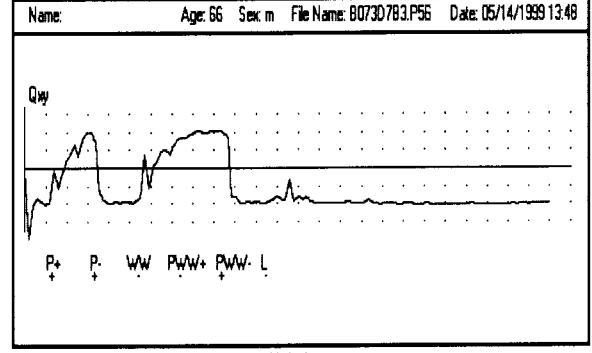
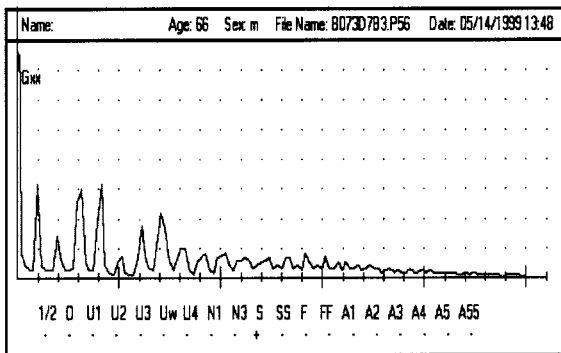
The final sample matched national demographic averages regarding racial makeup, was 60% male, and had a mean age of 61.3 years (Table 4). Sixteen percent of the patients had a history of myocardial infarction, 40% had hypertension, and more than 20% had diabetes (Table 4).

As stated previously, the device uses a discrete-Fourier transform signal-processing variant, and a series of six mathematic transformations. Predicate research and data collection efforts had established in the data base a set of thresholds for the indices of each of the six mathematic transformations to distinguish abnormal 3DMP electromechanic myocardial expressions from normal 3DMP expressions. The criteria of abnormality are empirically based on

### Graph Set A – Severe Coronary Disease



### Graph Set B – Moderate Coronary Disease



### Graph Set C – Normal Coronaries

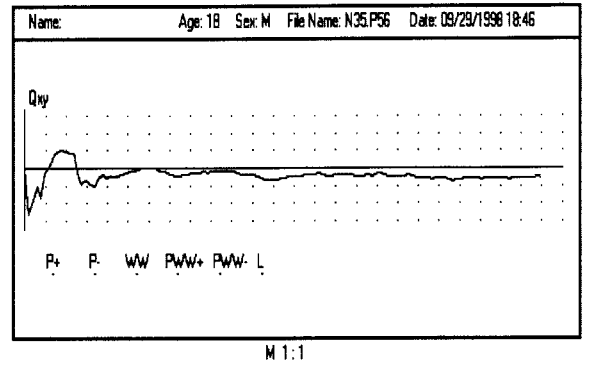
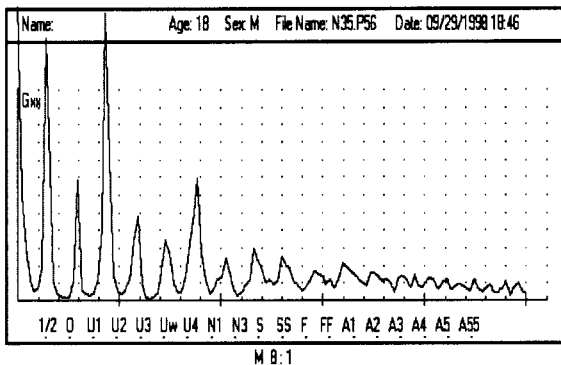


**Figure 5.** Comparative 3DMP graphic examples from normal to severe disease.

clinical diagnosis by a variety of conventional diagnostic procedures, principally coronary angiograms as the gold standard. The abnormalities stemmed from angiographically determined nonobstructive CAD (single-vessel arterial narrowing of  $\approx 40$ – $70\%$ ), left main narrowing of 40 to 50% to obstructive CAD (multivessel arterial narrowing of  $\approx 70$ – $100\%$ ), and 50 to 100% left main narrowing.

The biostatistical calculation was performed using Statistical Analysis System version 6.12 (SAS Institute, Cary, NC). Sensitivity for the study was 93.3%, positive predictive value was 91.2%, and specificity was 83% (negative predictive value, 86.7%)(Table. 3). When the sample was stratified by gender, results were similar. The 3DMP electrocardiogram sensitivities for single-, dou-

**TABLE 4**  
Baseline demographic characteristics

Characteristic	Number of patients*
Age (y)	
0-40	4.4 (6)
40-60	36 (49)
>60	59.6 (81)
Gender	
Male	60 (81)
Female	40 (55)
History	
MI	16 (22)
Smoking	42 (57)
Hypertension	39.7 (54)
Diabetes	
ID	3.7 (5)
NID	17.6 (24)
COPD	2.9 (4)
Hypercholesterolemia	4.4 (6)
Renal dysfunction	3.7 (5)
Anemia	5.9 (8)*
Electrolytes	
K <sup>+</sup>	5.1 (7)†
Na <sup>+</sup>	1.5 (2)‡
Cl <sup>-</sup>	22.8 (31)§
Electrocardiogram	
Normal	30 (41)
Abnormal	70 (95)

Data are % (n).

\*Percent of people with anemia.

†Percent of people with abnormal K<sup>+</sup>.

‡Percent of people with abnormal Na<sup>+</sup>.

§Percent of people with abnormal Cl<sup>-</sup>.

MI = myocardial infarction; ID = insulin dependent; NID = noninsulin dependent; COPD = chronic obstructive pulmonary disease.

ble-, and triple-vessel disease were 93.0, 96.3, and 97.1%, respectively.

Figure 6B presents the percentage of positive 3DMP electrocardiographic findings by comparison with percent arterial occlusion. The enhanced electrocardiogram detected abnormalities in 90% of patients subsequently found to have 50 to 70% narrowings by angiography. For patients with 40 to 50% narrowings, the 3DMP detected abnormalities in 75% of cases, which represents a significant increase in percent-positive 3DMP electrocardiogram tests compared with patients categorized with less than 40% narrowings. However, we also obtained abnormal readings in 22.2% of patients subsequently found to have normal coronary arteries and in 18% of patients found to have less than 40% stenosis of at least one major artery (Fig. 6B). Out of 43 patients with normal 12-lead electrocardiographic findings, 26 were angiographically positive for CAD (Table 5); the 3DMP electrocardiogram identified 19 of these 26 CAD patients.

## DISCUSSION

The advent of more accurate serologic and investigation techniques in the detection of subclinical CAD has spurred the improvement of diagnostic technologies. Database-driven, frequency/time-domain devices may provide a reliable, cost-effective alternative to current methodologies.

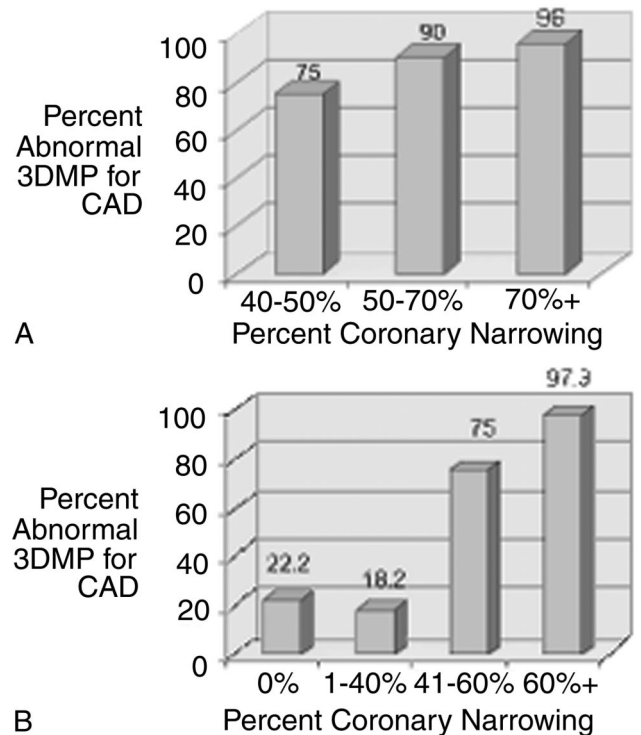


**Figure 6.** Percent of abnormal 3DMP expressions of various groups with varying degrees of coronary occlusions.

As in this investigation, the preliminary evidence that a device can identify the early onset of CAD, before clinical presentation, may provide preventive measures that reduce and delay the onset of a first myocardial infarct in patients with silent ischemia and smaller percent coronary narrowings. Our study was clearly limited by its small sample size, in which 34% of patients were determined to have normal coronary arteries by coronary angiograms. These patients may have had causes of myocardial dysfunction other than coronary artery ischemia. This group of patients provided the measures for calculating the meaningful specificities in identifying people who did not have anatomic abnormali-

**TABLE 5**

Percent coronary narrowing versus 3DMP differential diagnosis (CAD=OHD=Normal) versus 12 lead EKG undifferentiated diagnosis (normal and abnormal only)

Angiogram	3DMP (n)	Electrocardiogram (n)	
		Abnormal	Normal
Negative: 0% (n = 36)	Normal (3)	2	1
	CAD (8)	3	5
	OHD (25)	15	10
Negative: 0-40% (n = 10)	Normal (1)	0	1
	CAD (0)	0	0
	OHD (9)	5	4
Positive: 40-60% (n = 12)	Normal (1)	1	0
	CAD (8)	5	3
	OHD (3)	3	0
Positive: > 60% (n = 78)	Normal (2)	1	1
	CAD (76)	58	18
	OHD (0)	0	0

3DMP = digital database-driven multiphase electrocardiograph system; CAD = coronary artery disease; OHD = other heart disease.

ties. However, selection bias in all patients undergoing angiography to diagnose coronary arterial abnormalities was apparent. These patients may further be studied using intravascular ultrasound to determine their degree of intimal plaque formation or lack thereof.

As mentioned earlier, preliminary work on the device tested in the current study began in the 1970s and included canine left-anterior descending ligation and murine magnesium-sulfate toxicity.<sup>33,34</sup> The 3DMP electrocardiograph device detected the onset of the cardiac changes elicited by magnesium-sulfate injection upwards of 400% earlier than conventional electrocardiography. These reproducible results led researchers to pursue human cardiovascular studies. A subsequent pilot trial of three populations in Beijing showed, with significant sensitivity and specificity, that the 3DMP device was able to distinguish control patients with normal and abnormal electrocardiographic findings. A large-scale trial with 30 sites and 100 investigators was then conducted, thereby providing the foundation for the 21,000-patient database used to create the mathematic formulas used in the present study.<sup>35</sup>

The device's sensitive nature permitted the capture of only 68% of the population tested. Testers were blinded to differences in baseline risk profiles and demographics, making patient exclusion based solely on tracing quality objective. As described in Results, several factors contributed to difficulty in capturing artifact-free tracings. This aspect of the study may be perceived as a shortcoming, but physical surroundings are always a consideration with any sensitive diagnostic modality and must be minimized accordingly. The implementation of a Faraday cage (an examination room shielded with copper or copper-nickel alloy sheeting and earth grounded) will increase tracing acceptance (and was not available at the time this trial was conducted) because of its ability to minimize ambient electromagnetic interference. This is also a relatively cost-effective measure for small and large venues to incorporate. Other means of reducing rejection rates can also be easily implemented. For example, a clinical trial currently being conducted in Germany maintains less than 10% rejection rates without the use of a Faraday cage. This reduction is achieved merely by tending to small but important issues, such as consistently using a medical-grade electrical outlet and ensuring that electrocardiogram leads are not contiguous or abutting metal objects during testing.

Bias in this study was influenced by several factors. Thirty-four percent of patients who underwent angiography were found to have either angiographically normal coronary arteries or less than 40% diameter narrowing; these patients, who had positive 3DMP electrocardiographic findings, exhibited other myocardial diseases, including left ventricular hypertrophy, dilated cardiomyopathy, or valvular disorder. Eight patients were identified as having 3DMP abnormalities associated with CAD. These findings were considered false negative. Twenty-eight percent of patients were identified as having normal or OHD. These results were treated as true negative.

Previous investigations corroborate and reconfirm our use of 40% narrowing as the threshold for a positive result, though the reasoning for this device remains speculative.<sup>36–38</sup> These researchers surmise that oxidative stress resulting from activity of daily living may cause transient episodes where demand exceeds supply at 40% or greater coronary narrowing generates expressions registered on some or all of the six mathematically derived functions for the myocardium. The suggested compensatory arterial enlargement limit before atherosclerotic plaque formation compromises coronary blood flow has been confirmed to be a 40% narrowing, with considerable encroachment on the internal elastic lamina.<sup>39</sup> Intravascular ultrasonography would likely prove a more effective modality in future investigations to substantiate the capacity of the 3DMP to identify this threshold, though it has been indirectly supported through this investigation. As such, our representation of the data in Figure 6A was deliberate, in an effort to demonstrate this interesting result.

It is intriguing to observe that after analyzing the entire sample, three patients for whom the expert computer system generated false-negative results angiographically demonstrated collateral growth. Others had some degree of low-grade narrowing evident on the angiograms, without systemic or confounding causes. This discovery was made after a double-blind protocol was opened, and is therefore not a part of the formal trial.

On further examination, irregularities in three graphs emerged. Power output on the power-spectrum graphs (Gxx and Gyy) shifted approximately 2 or 3 Hz toward the higher end of the frequency spectrum. This redistribution of power was therefore reflected in a peak-amplitude change (i.e., peaks three, four, five, and six became larger than peak one). These peaks are normally much less expressed than the first fundamental peak. Patient coherence graphs also showed a greater number of peaks contained within the first 5 Hz. The amplitude changes and power shifts seen in these graphs never exceeded the software's predetermined threshold values, and therefore never generated a positive index. This result is logical in that the original database studies did not account for collateral arterial growth. No established patterns had been examined closely and tested empirically. Because only six patients were noted to have angiographic evidence of collateral growth or uncomplicated, stable, lower-grade narrowing, it is possible that this correlation is spurious and obviously necessitates rigid scientific investigation.

Our demonstration of certain peak ratios deduced from the 12-lead electrocardiogram, in concert with specific indices on the system, may allow researchers to differentiate CAD and OHD. Congestive heart failure (not the OHD groupings found in Figure 3 and Fig. 4), may also be included in future research. Although much additional study is needed to fully exploit this possibility, the initial results coincide with what was found historically and clinically. In addition, data collected during this study are presently being gathered for postreperfusion studies to assess the device's efficacy in accurately tracking postprocedure patho-

logic resolution. Other multicenter studies addressing these issues (both short and long term) have also been planned, specifically at Herzzentrum Siegburg in Siegburg, Germany. A study to compare 3DMP with sestamibi has also been planned.

The ultimate goals remain the exploration of the pathogenesis of CAD, secondary only to reliable, noninvasive, early detection and prevention of CAD for subcritical narrowings. The 3DMP electrocardiograph may detect altered electrical patterns resulting from repeated ischemic insult (both acute and chronic) on the myocardium, stemming from the activities of daily living. It is anticipated that future work will afford the device the ability to “see” the intermittent dynamic changes that may coincide with plaque instability, from a conductive perspective and in real time. Although immature, unstable plaques are vascular phenomena, and their displacement or occlusion has a direct and deleterious impact on myocardial perfusion.

## CONCLUSIONS

The 3DMP resting electrocardiograph system coupled with 12-lead electrocardiography has quantifiable diagnostic utility in identifying abnormalities associated with the presence of CAD. Early diagnosis of low-grade, subcritical, and silent lesions is possible.

## REFERENCES

- American Heart Association. Cardiovascular disease statistics [American Heart Association Web site]. Available at: <http://www.americanheart.org>. Accessed November 12, 1996.
- Hurst JW. *Ventricular Electrocardiography*. 1st ed. New York, NY: Gower Medical Publishing, 1991.
- Zir LM, Miller SW, Dinsmore RE, et al. Interobserver variability in coronary angiography. *Circulation* 1976;53:627–632.
- Galbraith JE, Murphy ML, de Soya N. Coronary angiograms interpretation. Interobserver variability. *JAMA* 1978;240(19):2053–2056.
- Little WC, Constantinescu M, Applegate RJ, et al. Can coronary angiography predict the site of a subsequent myocardial infarction in patients with mild-to-moderate coronary artery disease? *Circulation* 1988;78:1157–1166.
- Holmyang G, Fry S, Skopicki HA, et al. Relation between coronary steal and contractile function at rest in collateral-dependent myocardium of humans with ischemic heart disease. *Circulation* 1999;99:2510–2516.
- Morton BC, Higginson LA, Beanlands DS. Death in a catheterization laboratory. *CMAJ* 1993;149:165–169.
- Jansson K, Fransson SG. Mortality related to coronary angiography. *Clin Radiol* 1996;51:858–860.
- Bach R, Espinola-Klein C, Ozbeck C, et al. Complications after coronary angiography and balloon dilatation. *Dtsch Med Wochenschr* 1993;118:1669–1776.
- Morton BC, Higginson LA, Beanlands DS. Death in a catheterization laboratory. *CMAJ* 1993;149:165–169.
- Little WC, Constantinescu M, Applegate RJ, et al. Can coronary angiography predict the site of a subsequent myocardial infarction in patients with mild-to-moderate coronary artery disease? *Circulation* 1988;78:1157–1166.
- Wexler L, Brundage B, Crouse J, et al. Coronary artery calcification: pathophysiology, epidemiology, imaging methods, and clinical implications. AHA medical/scientific statement. *Circulation* 1996;94:1175–1192.
- Fuster V, Lewis A. Connor memorial lecture: mechanisms leading to myocardial infarction. Insights from studies of vascular biology [erratum appears in *Circulation* 1995;91:256]. *Circulation* 1994;90:2126–2146.
- Smith SC Jr, Greenland P, Grundy SM, Prevention Conference V. Beyond secondary prevention: identifying the high-risk patient for primary prevention. Executive summary. Proceedings of the American Heart Association conference. *Circulation* 2000;101:111–116.
- Deanfield JE. Total ischemic burden in patients with coronary artery disease. *Cardiovasc Drug Ther* 1990;4(Suppl):833–839.
- Shea MJ, Deanfield JE, Wilson R, et al. Transient ischemia in angina pectoris: frequent silent events with everyday activities. *Am J Cardiol* 1985;56:34E–38E.
- American Heart Association. Cardiovascular disease statistics [American Heart Association Web site]. Available at: <http://www.americanheart.org>. Accessed November 12, 1999.
- Kajinami K, Seki H, Takekoshi N, Mabuchi H. Coronary calcification and coronary atherosclerosis: site by site comparative morphologic study of electron beam computed tomography and coronary angiography. *J Am Coll Cardiol* 1997;29:1549–1556.
- Bach R, Espinola-Klein C, Ozbeck C, et al. Complications after coronary angiography and balloon dilatation. *Dtsch Med Wochenschr* 1993;118:1669–1676.
- Menown IBA. Early diagnosis of acute myocardial infarction in patients presenting with ST depression only on 12-lead electrocardiogram. Scientific sessions of the American Heart Association. November 8–11, 1998; Belfast, Northern Ireland.
- Huikuri HV, Valkama JO, Airaksinen KE, et al. Frequency-domain measures of heart rate variability before the onset of non sustained and sustained ventricular tachycardia in patients with coronary artery disease. *Circulation* 1993;87:1220–1228.
- Menown IBA. Early diagnosis of acute myocardial infarction in patients presenting with ST depression only on 12-lead electrocardiogram. Scientific sessions of the American Heart Association. November 8–11 1998; Belfast, Northern Ireland.
- Huikuri HV, Valkama JO, Airaksinen KE, et al. Frequency-domain measures of heart rate variability before the onset of non sustained and sustained ventricular tachycardia in patients with coronary artery disease. *Circulation* 1993;87:1220–1228.
- Ivanov GG, Kovtun VV, Kago M, Titomir LI. High-resolution electrocardiograph abnormalities as possible indexes of electrical instability of the myocardium. *Can J Cardiol* 1996;12:53–58.
- Prasad K, Gupta MM. PISA: a new non-invasive method for early detection and quantification of heart disease. *Adv Myocardiol* 1:287–312. Available at: Aspect Medical Systems Web site: <http://www.aspectms.com>.
- Aspect Medical Systems. Home page of Aspect Medical Systems. Available at: <http://www.aspectms.com>. Accessed November 12, 1999.
- Bonato P, Bettini R, Speranza G, et al. Improved late-potential analysis in frequency domain. *Med Eng Phys* 1995;17:232–238.
- Feng GQ, Jing-Liang M. A theoretical model for dynamics of heart and the multiphase information analysis of EKG. In: Proceedings of the Third International Symposium on Biomedical and Rehabilitation Engineering; Shanghai, China, November 1987; 39–44.
- Wiener N. *Nonlinear Problems in Random Theory*. Cambridge, MA: MIT Press, 1958.
- Wiener N. *Cybernetics*. 2nd ed. Cambridge, MA: MIT Press, 1961.
- Winfree AT. Biological rhythms and the behavior of populations of coupled oscillators. *J Theor Biol* 1967;16:1542.
- Alderman E, Stadius M. The angiographic definitions of the bypass angioplasty re-vascularization investigation. *Coron Artery Dis* 1992;3:1189–1207.
- Feng KC. A theoretical model for dynamics of heart and multiphase information analysis of EKG. In: Proceedings of the Third International Symposium on Biomedical and Rehabilitation Engineering; November 1987; Shanghai, China. Abstract C39.
- Feng KC. Some studies on the EKG of magnesium ion toxication model. In: Proceedings of the Third International Symposium on Biomedical and Rehabilitation Engineering; November 1987; Shanghai, China. Abstract C129.
- Feng KC. *EKG and EEG Multiphase Information Analysis*. 1st ed. New York, NY: American Medical Publishers, 1992.
- Glagov S, Weisenberg B, Zarins C, et al. Compensatory enlargement of human atherosclerotic coronary arteries. *N Engl J Med* 1987;316:1371–1375.
- Losordo D, Rosenfield K, Kaufman J, et al. Focal compensatory enlargement of human arteries in response to progressive atherosclerosis. In-vivo documentation using intravascular ultrasound. *Circulation* 1994;89:2570–2577.
- Nissen S, Yock P. Intravascular ultrasound. Novel pathophysiological insights and current clinical applications. *Circulation* 2001;103:604.
- Glagov S, Weisenberg B, Zarins C, et al. Compensatory enlargement of human atherosclerotic coronary arteries. *N Engl J Med* 1987;316:1371–1375.